

From Optimal Structural Configuration to Truss Optimization

C.Y. Lin, J.F. Chang and J.Y. Juang
Department of Mechanical Engineering
National Taiwan University of Science and Technology
Taipei, Taiwan R.O.C.

Abstract

An integrated truss design methodology based on homogenization-based topology optimization is proposed. After performing continuum topology optimization to obtain the optimal structural configuration, in the case that the percentage usage of the materials is low, the methodology can automatically proceed to the truss optimization based on the model, and achieve the optimum truss structure meeting the constraints. The three-dimensional continuum topology obtained from the homogenization-based topology optimization will be automatically converted to the truss model by using the unique node and bar detection techniques, and then the truss optimization can be autonomously executed so as to obtain the optimal truss design meeting all constraints.

Keywords: topology optimization, truss structure, automated structural design process, three-dimensional thinning, automated node search, material usage ratio.

1 Introduction

Michell [1] proposed a simple design of the lightest frame on the concept of structural optimization, followed by the emergence and development with the computer. Many scholars have made a number of structural optimization theories, mainly on the size optimization. Later, the successful development of the computer analyzing software on finite element algorithm greatly improved the efficiency of the structural analysis, which rapidly boosted the development of the structural design optimization from the field of the size optimization to the field of the shape optimization. Both shape and size optimization will require a proper initial design structure. Traditionally, the design models are mostly based on experiences, which often lead to poor final designs. As a result, the concept regarding the topology optimization [2] [3] got brought up here and there in the academic field, the use of

topology optimization method that is able to first obtain a better design basis, as the size optimization [4] and shape optimization [5] for the initial design structure. However, in today's rapid paces for the development of the modern technology, everything has to be time-concerned. To shorten the design process and reduce the time costs and the expenses, scholars have proposed a number of systematic design methods.

Papalambros et al. [6] proposed the integrated structural optimization system (ISOS), by combining the topology optimization and the structural shape optimization, a complete set of structural design methods was hence established. This approach used of the homogenization theory [7] to perform the topology optimization. During the process, with a large number of design variables, more amount of time has to be taken to finish the analyses required in optimization. Furthermore, in the follow-up structure and shape optimization, the need to manually define the structural geometry and shape variables is set as their defects. Based on the above defects, many scholars dedicated themselves in order to optimize the integration of topology and shape optimization of the architecture, along with the development of an integrated topology optimization, shape optimization and size optimization of fully integrated design automation system [8] - [11].

Generally speaking, the industrial designs are likely to be constrained according to the allowable stress of the materials. However, most of the topology optimization only uses the compliance of structure as the objective function, with the use of materials limited to the method, which often results in infeasible designs with the actual situation. Thus, Lin and Hsu [12] developed a stress or displacement-based iterative topology optimization method, which incorporated the sequential linear programming [13] as the optimization tool, the compliance as the objective function, and an adjustable material usage rate based on the difference between the maximal stress or displacement in the current structure compared to the allowable stress or displacement of the topology. Combined with the computer vision processing technology, an integrated topology optimization and shape optimization for automatic design system becomes possible.

However, when the optimal topology has a more sturdy appearance, it is able to produce an optimal continuum structure out of the shape optimization. When the topology is slim, it would be more properly handled if the topology is converted into a relatively discrete structure. Paris et al. [14] proposed the local stress and global stress constrained topology optimization. Although the artificial parameters are not necessary to be defined for the local stress, but the stress will be limited to pre-defined design points, and the number of variables will affect the computational costs more. By punishing the intermediate density, the resultant configuration will have a truss-like structure. Rong et al. [15] proposed the topology optimization on the limit of the stress and the need for the initial configuration. When the iterations converge more frequently, its configuration will be similar to truss structure.

In recent years, many scholars have devoted into the study of discrete structures, most of the structure are directly assumed as a discrete truss structure at

the beginning of the design process. For the truss structure of the topology optimization methods, Kirsch [16] proposed the ground structure method, which defines all possible structures into a two-force discrete bar combination. Then the optimality criteria method or the linear programming method was adopted to remove unnecessary bars, simultaneously to adjust the size of bars. This method requires the designer to set in advance a fixed node and bar in the design space, the morphology obtained by the previous approach will be significantly influenced by the designers' past experiences. Lu et al. [17] presented the method to transform the concrete structure of the pressure rod obtained by the topology optimization into the structure of the corresponding compression truss rod model. But in transferring the continuum topology into a truss structure, it requires a manual operation. Based on the above defects, Zheng [18] used the computer vision technology to automatically thin the similar two-dimensional truss topology, and refine the results to determine the nodes and the truss bars to enable a successful conversion to truss structure. Shen [19] proposed the two-dimensional truss design optimization platform which can obtain the optimal truss structure.

Figure 1 shows the integrated structural design system and points out that before design problems, there is no default setting to the continuum as for a discrete structure analysis, but it will be determined by the stress-based topology optimization of iterative design topology obtained after the amount of usage of its materials. If the material usage is greater than a certain value, the system will automatically optimize the shape of the continuum, if less than a certain value, it will perform discrete truss structure optimization.

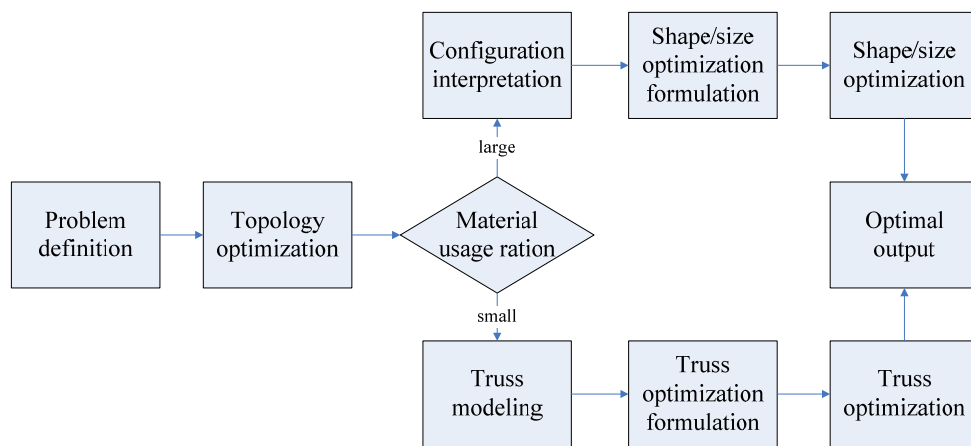


Figure 1: The integrated structural design system

However, in practical engineering applications, most examples are of three-dimensional structures. There are some constraints concerning the working range of the optimum design platform for two-dimensional truss structures. Converting the optimal configuration resulted from the topology optimization to a truss model, the challenge is to identify the nodes and bar members that form a truss from the continuum structure in an automated manner. Borrowed from image process

techniques, the method to thin a two-dimensional topology is well established. One of the most commonly adopted ones would be the Zhang-Suen algorithm by Zhang et al. [20]. As for the thinning for the three-dimensional topology, there are also many scholars involved in recent years. Ma et al. [21] proposed a three-dimensional parallel thinning method, defining 38 kinds of edge element model. Wang et al. [22] [23] proposed a series of adjustment strategy for this model, and Wang and Basu proposed the refinement method. In addition, this research incorporates the two-dimensional Zhang-Suen algorithm based refinement method. The authors present a revised method, which is based on the advantages of the Wang and Basu method, to combine the advanced three-dimensional refinement, coupled with the automatic node search and the bar connectivity determination technology. The unique approach can successfully convert the structural configuration into the truss structure, serving as the initial structural model of the subsequent truss optimization.

In general, when the material usage of the optimal topology is low, it is closer to the appearance of discrete truss structures compared to continuum structures. This paper presents an integrated approach to convert the optimal topology of continuum structures into a three-dimensional truss topology based on the unique 3D thinning algorithm and node and bar connectivity detection techniques, and then conduct the truss optimization in a fully automated manner. The proposed method is tested in a number of 2D/3D engineering structural optimization problems with success.

2 3D structure thinning

After the optimal configuration is obtained by topology optimization, a 3D thinning process to change the configuration into a skeleton type structure will be needed so that the effective subsequent node search and bar connectivity check algorithms can be performed. These algorithms form the basis of the automated construction of a truss model based on the optimal configuration.

2.1 Lin and Chang method of three-dimensional refinement

As Wang and Basu refinement method is ineffective in some cases, the Zhang-Suen thinning algorithm processed in the 2D image plane has better outcome. The new proposed 3D thinning algorithm, referred to Lin and Chang method, an extension of the Zhang and Suen method to work in 3D space, will be discussed in details below.

First, we define $3 \times 3 \times 3$ elements of the nine planes through the center of the 3×3 mask as shown in Figure 2. Then as suggested by Zhang-Suen algorithm, when n planes out of the nine planes meet the deletion criteria, the central element will be removed. According to the tests, n equal to 6 will lead to a better refinement results. In addition, we will implement the revised Wang and Basu refinement method to detect the continuity and symmetry of a fixed set of elements. All elements in the structure will be repeatedly checked and deleted when necessary until convergence.

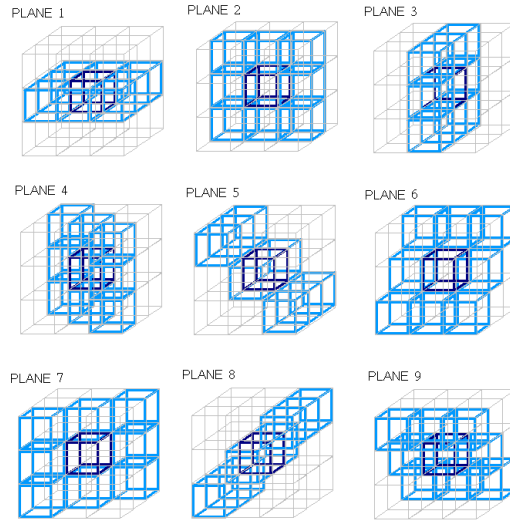


Figure 2: $3 \times 3 \times 3$ mask passing P1

2.2 Advanced thinning algorithm

Firstly, we use the Wang and Basu refinement method and Lin and Chang refinement method to perform the thinning process on two binary structures as shown in Table 1. Table 1 shows the results of two approaches.

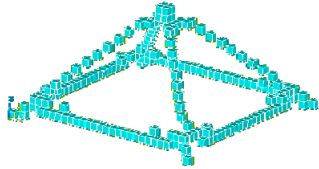
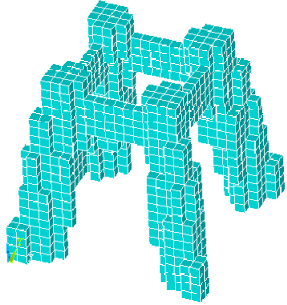
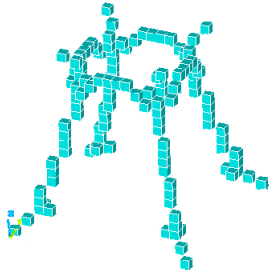
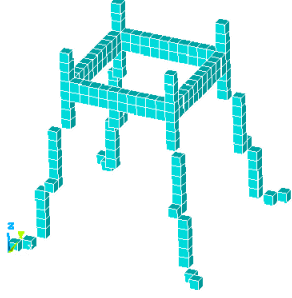
Initial Binary Structures	Results of Wang and Basu Thinning Method	Results of Lin and Chang Thinning Method
		
		

Table 1: Comparison of Wang and Basu and Lin and Chang methods

We can find the following two conclusions:

- (1) Wang and Basu refinement method has a good effect at the intersection of bars of the structure with few empty elements, but the surface of the bars seems quite rough.

(2) Lin and Chang refinement method performs very good in simple structures, but empty elements occur in more complex structures.

This paper will use Wang and Basu method mainly, and assisted by Lin and Chang method, to refine the structures. Of course, in the process of refining the structure, the identification techniques for the continuity of the fixed elements, and the symmetry of the structure have been also implemented, which is referred to as the advanced three-dimensional thinning technique (ATDT). The flowchart of the technique is shown in Figure 3. Figure 4 shows the results of implementing the advanced three-dimensional thinning technique (ATDT)

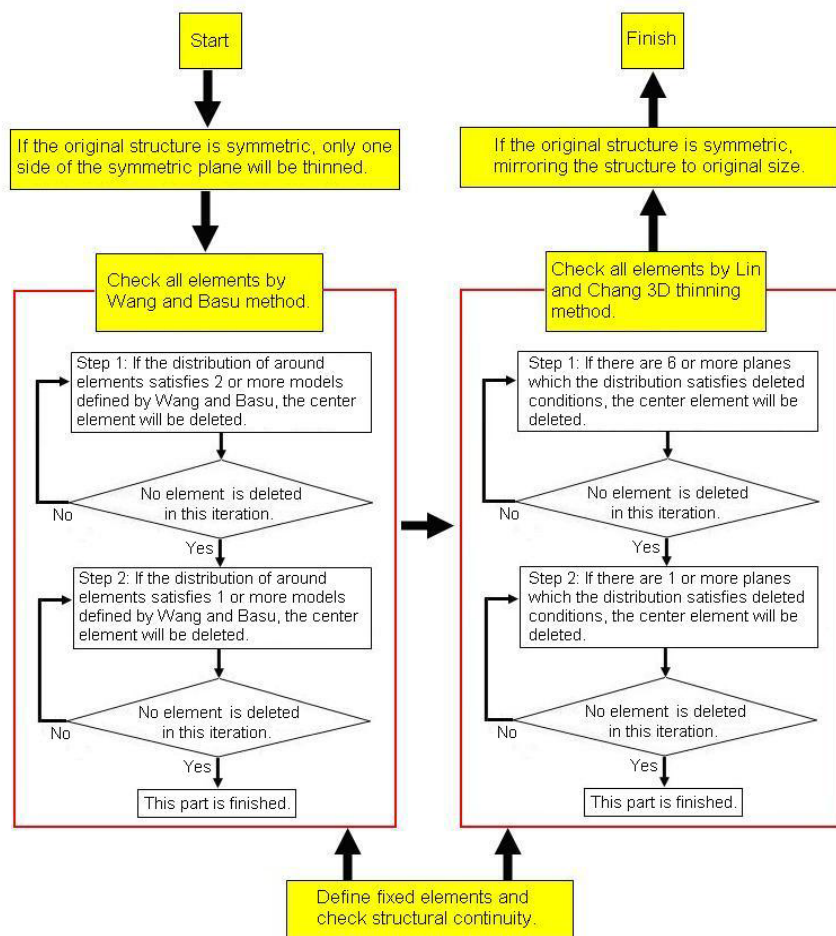


Figure 3: Flowchart of advanced 3D thinning techniques

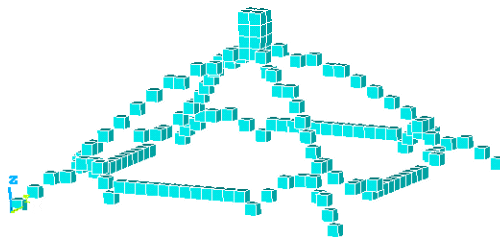


Figure 4: Output of advanced 3D thinning techniques

3 Automatic truss model generation

By using the iterative topology optimization method, a binary topology meeting the preset stress or displacement constraints will be obtained. If the material usage is low, the structure will resemble a truss structure. The three-dimensional structure refinement technology is now the key technique to transform a 3D structure into a 3D truss. After the truss model is defined, the subsequent truss optimization can be performed as shown in Fig. 5. Combining with image processing techniques [24] and the automatic search of the proposed nodes and connecting rods, the truss model will be generated.

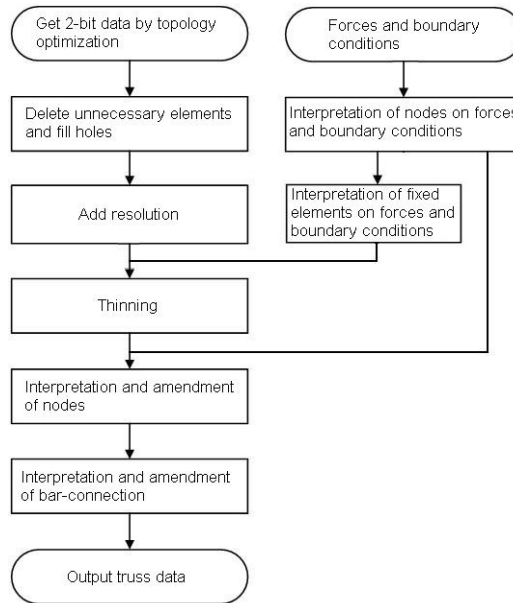


Figure 5: Flowchart of 3D truss structure model building

3.1 Data pre-processing

The binary image obtained after the topology optimization sometimes will have empty holes, or disconnected elements, which may consequently cause a failure of the truss model generation. Pre-processing is then necessary before thinning process.

3.1.1 Removal of the noisy elements

First, we define a $3 \times 3 \times 3$ mask, and scan all elements one by one. P2 ~ P27 represents the elements surrounding the mask. As shown in Figure 6, if the element P1 to be scanned is 1 and the surrounding elements, P2 ~ P27 are all 0, the P1 element is considered as an isolated noise. If P1 is not an element on the boundary, and the sum of its peripheral elements P2 ~ P27 to 1, P1 is deemed as an extended element. These two elements in the structure are not preferred, therefore they should be removed. These unwanted elements are identified by arrows as in Figure 7.

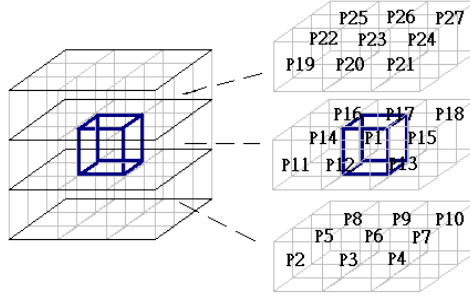


Figure 6: $3 \times 3 \times 3$ mask

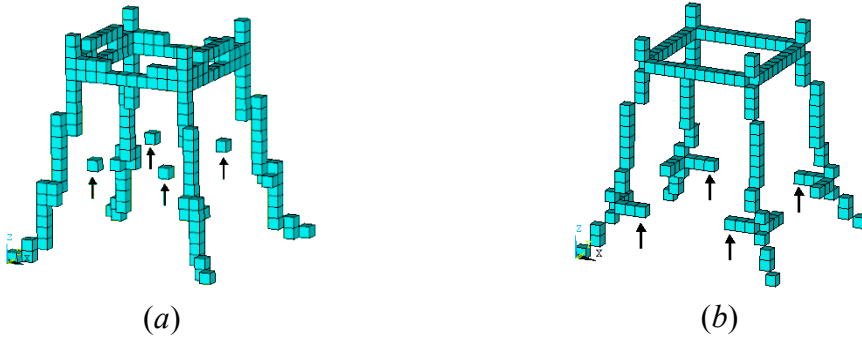


Figure 7: Two types of noisy elements, (a) isolated, (b) extended

3.1.2 Hole fixing

First, we define the nine 3×3 planes passing the central element P1 inside the $3 \times 3 \times 3$ mask as shown in Figure 8.

- (1) If one of 9 planes whose four surrounding elements exist, the central element, P1, is deemed as a hole. Figure 8(a) uses the Plane 6 in Figure 2 as example, the gray elements are all 1, which surrounds the hole element P1.
- (2) Figure 8(b) represents the direction of the arrow perpendicular to the plane, and the direction of the pixel and three pixels on the plane to form a loop, so that the holes can be regarded as P1 .

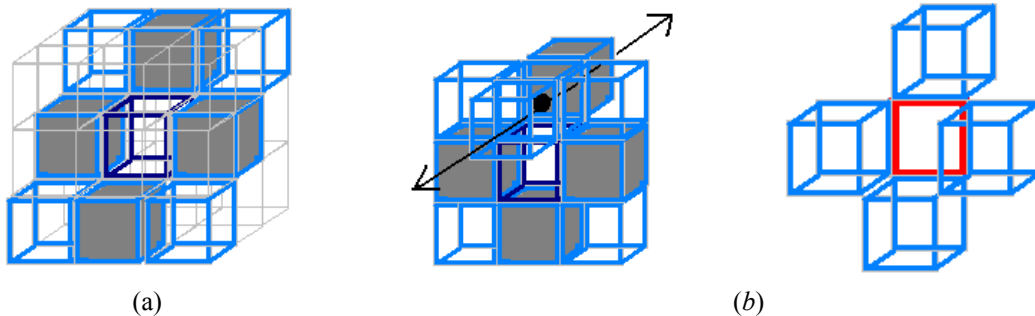


Figure 8: Void in 3D structure

The $3 \times 3 \times 3$ mask is used to scan all the elements one by one. If the element P1 is an empty element 0, and its surrounding elements meet the above conditions,

P1 is deemed as an empty hole. Subsequently, the element of P1 will be changed from 0 to 1.

3.1.3 Improve the resolution and refinement process

The structure obtained after the topology optimization needs to be checked and all nodes and connecting bars should be properly identified so as to generate a truss design. But since the structural configuration has low resolution, it is very difficult to implement the automated node and bar checking algorithm. Therefore, the original structure needs to be transformed into one with a higher resolution, and then the 3D thinning technique is applied to get the node and bar information.

Using the three-dimensional fixed column structure under 4 loads as in Jacobsen et al. [25] as an example, Figure 9(a) shows the structure represented as a coarse mesh in which node positions at the bottom are difficult to be identified. Figure 9(b) shows the same structure but now with 27-time higher in resolution. Figure 9(c) shows the structure undergoes the 3D thinning process.

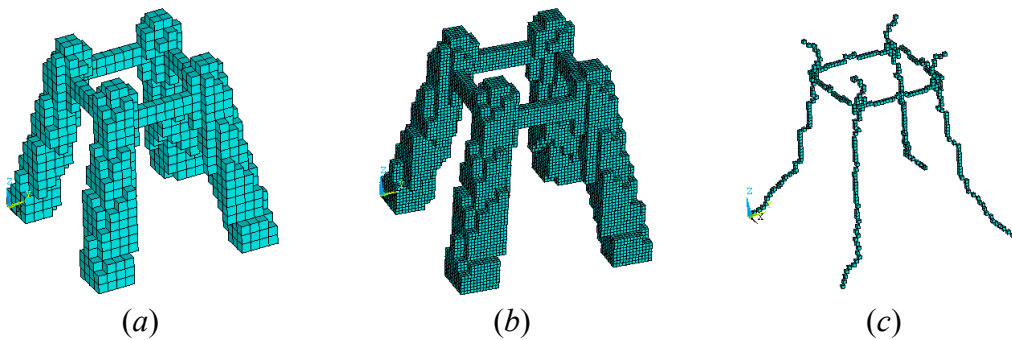


Figure 9: (a) Coarse mesh structure, (b) Refined mesh structure, (c) The thinning result

3.2 Node and fixed element criteria

The fixed elements to the ground and elements under external loads need to be reserved before performing the 3D thinning process, and the corresponding nodes should be identified first.

3.2.1 Fixed end elements and elements under external force

Node location is force coordinates, compared with the coordinates of the fixed elements of the nearest element. If two or more fixed elements, then determine the coordinates of the design space is located in the midpoint position of the axis, if the elements of this direction are set at a fixed element, if not, then it is closer to the edge of the element. Figure 10 is a design space of the upper surface, F1 and F2 for the two force points, including two F1 x and y axes in the mid-point position, so near the four elements are set to a fixed element, and F2 were not located mid-point location in either direction, so only the elements closest to the edge of the dark blue

set of fixed elements. Fixed end nodes to determine the location and method of the fixed elements of the same side with the force.

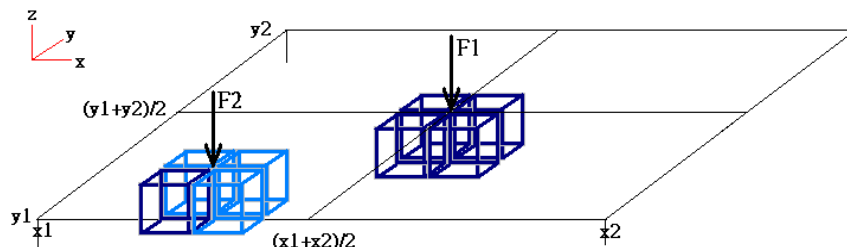


Figure 10: A design space of the upper surface

3.2.2 Fixed line and fixed surface

First, we find out the adjacent elements with fixed line, and classify the connected elements to the same group. If there is the element of any group close to either end of fixed line, then the end of fixed line set to a node and the element set to the fixed element, as shown in the case1 of Figure 11. If there is no element of any group close to either end of fixed line, then the midpoint of fixed line set a node and the adjacent element with the node set the fixed element. If there are two adjacent elements, the judgment method is the same as elements under external force, as shown in the case2 of Figure 11. As for the nodal location and fixed element of fixed surface, the judgment method is similar to fixed line. The difference is more than the judgement of one direction.

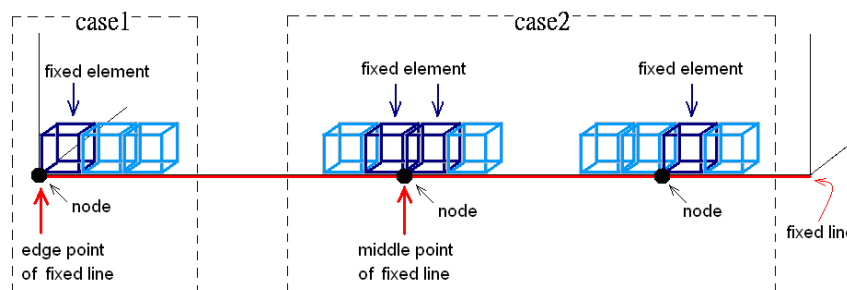


Figure 11: Determination of nodal position and fixed elements on the fixed line

3.2.3 Judged the node strategy

If the node of a three-dimensional space did not locate in the fixed end elements and elements under external force, there are at least three rods connected around the node. Therefore, the $3 \times 3 \times 3$ mask is used to scan all the elements and to determine the distribution of the surrounding elements for the space. If the situation is meet one of the below conditions, the center of the element set a node.

- (1) The line is connected with the central element and the surrounding elements, and calculated the included angle between these lines. If the included angle is less than 50° , the elements are classified as the same group. The total number of

groups is more than three, the center of the central element will be judged as a node. For example, Figure 12, there are three groups for the included angle is less than 50° , namely the included angle is 35.26° between L1 and L2, the included angle is 45° between L2 and L3, and the included angle is 35.26° between L4 and L5. Consequently, the first group is q1, q2 and q3, the second group is q4 and q5, and q6 is the third group. The center of central element P is deemed as a node.

- (2) According to the tests, when the number of surrounding elements is more than eight, although it only divided into two groups for the grouping method of (1). The center of central element is still deemed as a node, as shown in Figure 13.

Figure 9(c) uses the judgment method of 3.2.1 - 3.2.3, it can get the map of the nodal location, as shown in Figure 14.

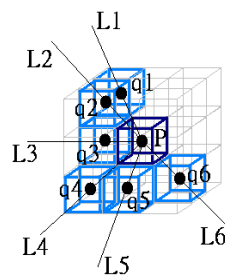


Figure 12: Nodal criteria – the included angle and grouping of surrounding elements

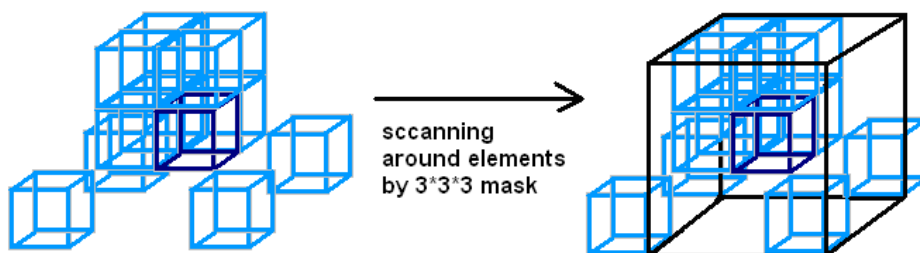


Figure 13: Nodal criteria – surrounding elements are more than 8

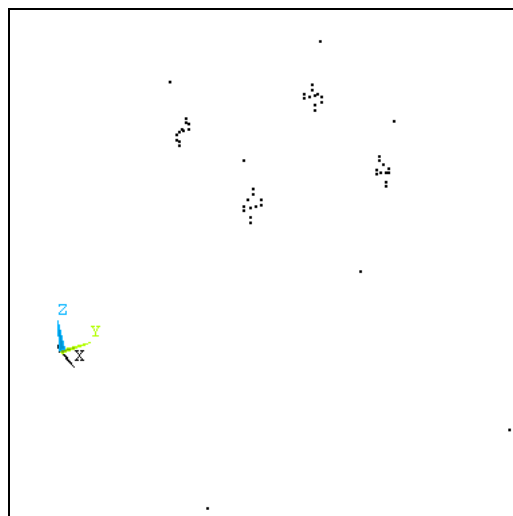


Figure 14: Nodal positions

3.2.4 The correction strategy of the adjacent nodes

We can get a lot of nodes through the judgment method of 3.2.1~3.2.3, but some of these nodes maybe very closely. In order to remove the redundant nodes, we define a searching radius (SR). We used a node as the center and SR as the radius to draw the sphere. If there are any nodes within the sphere, it will be classified the same group. If SR is very small, it will remain many nodes. If SR is very big, it will remove the correct nodes. According to the tests, we can get the empirical equation of SR, as shown in (1).

$$SR = \frac{L_x + L_y + L_z}{25} \quad (1)$$

where L_x , L_y and L_z represent the length in the x, y and z-direction of design space.

After the grouping finish, we detected each group whether fixed end elements or elements under external force. If so, we removed other nodes except fixed end elements or elements under external force. If not, the judgment method is as follows:

- (1) There is only one node within the group, it will be as a node.
- (2) There are more than two nodes within the group, and then we calculated the average of the coordinates of all nodes as the new coordinates. We calculated the distance from each node to the new coordinates, and then took the node of the shortest distance as node of the group. If there are more than two nodes of the shortest distance, and then took the average of them as node of the group.

3.3 Judged the bar connectivity

We judged the connectivity relationship after getting the coordinate and number of each node. The method described in detail as follows:

(1) Judgement strategy

First, we calculated the coordinates of trisection points for any two nodes. We used the trisection points as the center, and built the cube mask of the side L , respectively. Each mask is detected whether element is existed. There is bar connectivity between the nodes if two of three masks are detected element.

The masks of no.1 and no.3 are detected element, as shown in Figure 15. There is bar connectivity between the nodes of A and B. According to the tests, we can get the empirical equation of L , as shown in (2).

$$L = \frac{L_x + L_y + L_z}{45} \quad (2)$$

where L_x , L_y and L_z represent the length in the x, y and z-direction of design space.

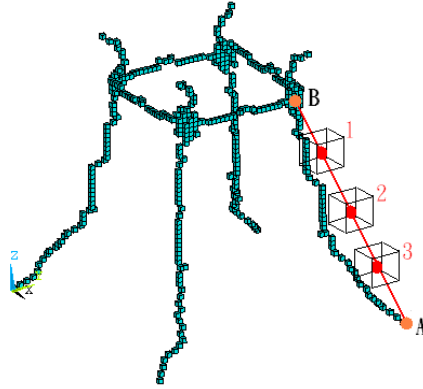


Figure 15: Determination of bar connectivity

(2) The correction strategy of adjacent bar connectivity

When all possible connection bars are obtained, we detected whether some bars misjudged due to close relationship of the included angle. In Figure 16, A, B, C, D and E are some nodes of the structure, and \overline{AB} , \overline{BC} , \overline{AC} , \overline{CD} and \overline{CE} are some connection bars. We can find the included angle of \overline{AB} , \overline{AC} , \overline{CD} and \overline{CE} are small, so the bars of \overline{AB} and \overline{CD} are misjudged and corrected.

First, the length and direction of each bar connectivity was recorded. Then we discussed the all bar connectivity of each node in order, the bar of the shortest length is as a benchmark. We calculated the included angle between the benchmark and the other bars. When the included angle is less than 20.5° , and then removed the bar. Otherwise, the bar connectivity will be retained.

The shortest bar is selected as a benchmark in the retained bar and calculated the included angle between the benchmark and the other bars. Repeat the above steps until all connected bars of the node are determined. The included angle of 20.5° is empirical value.

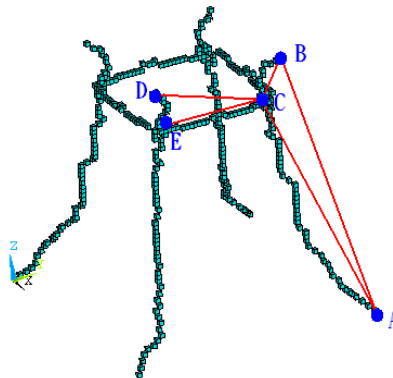


Figure 16: Misjudged redundant bars

4 Case Study

In this paper, we use the three-dimensional fixed beam with two loads designed by Jacobsen et al. [25], as the object of analysis and discussion. Design space dimensions and the cantilever force position are shown in Figure 17. The length is

60 in, the width is 80 in, and the height is 50 in. The Young's modulus of the material is 210,000 psi. The Poisson's ratio is 0.3. Two horizontal forces of 90,000 lb are loaded at the middle of the free end. The allowable stress value is 1,500 psi. The initial material usage is 25%.

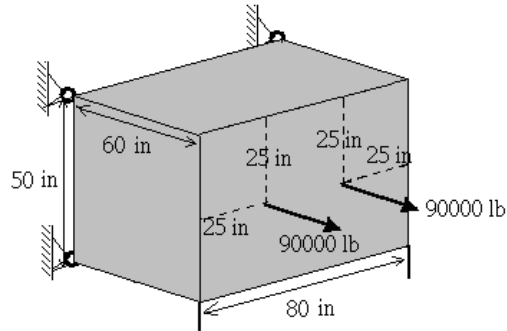


Figure 17: Design space of the 3D cantilever beam under two horizontal loads

The material usage ratio for the initial structural configuration is 20% material, and at the end of the topology optimization, the ratio drops into 6%. To tackle the problem that the stress levels in some elements exceed the allowable stress, the structure (8% material usage ratio) in the 5 previous iterations is implemented with binarization. The result is shown in Fig. 18(a). The structural confirmation after going through the proposed three-dimensional refinement process can be seen in Figure 18(b). The automated node determination strategy located 6 nodes in the design space as shown in Figure 18(c). The bar connectivity bar checking algorithm defines the truss, as shown in Figure 18(d). Finally, all the information about the truss is listed in an input file for analysis as shown in Figure 19.

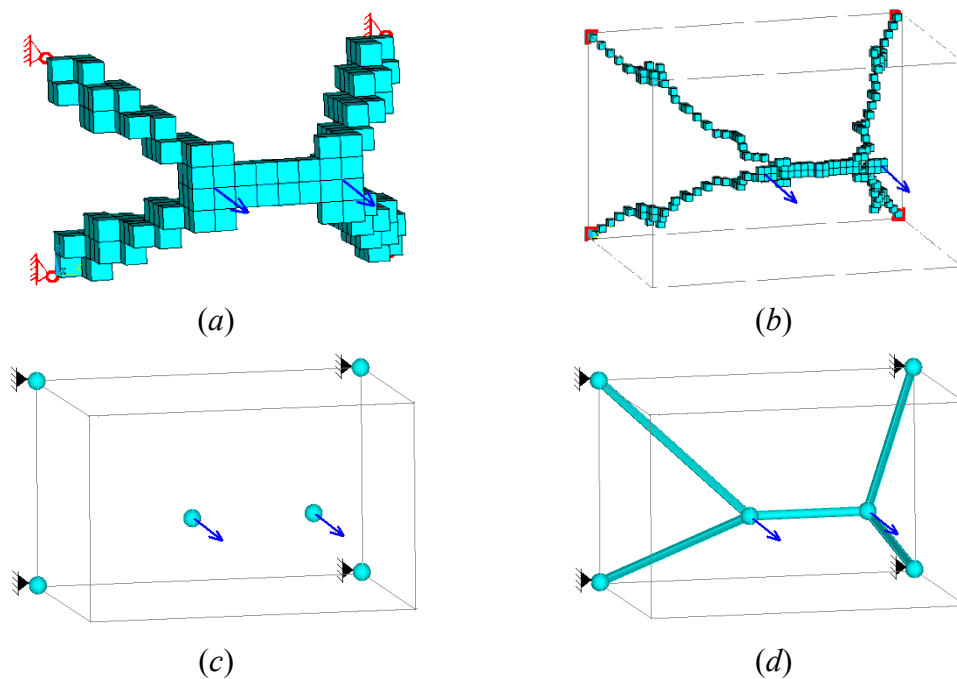


Figure 18: (a) Binary structure, (b) Skeleton after thinning, (c) Nodal positions, (d) Bar connectivity.

```

OPTION=1
INPUT
TITLE=BAR_TRUSS
JOINT LOCATIONS
1, 60.000, -15.000, 25.000
2, 60.000, 15.000, 25.000
3, 0.000, -40.000, 0.000
4, 0.000, 40.000, 0.000
5, 0.000, -40.000, 50.000
6, 0.000, 40.000, 50.000
*
ELEMENT LOCATIONS
SEC= 1
1, 1, 2
SEC= 2
2, 1, 3
SEC= 3
3, 1, 5
SEC= 4
4, 2, 4
SEC= 5
5, 2, 6
*
SECTION PROPERTIES
1, 1
2, 1
3, 1
4, 1
5, 1
MATERIAL PROPERTIES
1, 210000
*
APPLIED FORCES
1, 1, 90000.000
2, 1, 90000.000
*
CONSTRAINT DEFINITIONS
3, 1 2 3
4, 1 2 3
5, 1 2 3
6, 1 2 3
*
EXIT
SOLVE
DISPLACEMENTS
STRESSES
END

```

Figure 19: Output of the definition of the 3D truss

5 Conclusions

An optimal structural configuration with a low material usage ratio will be more similar to a truss structure than a continuum structure. This paper presents a set of

unique techniques to autonomously transform the optimal configuration into a truss design model which can serve as a great design model for subsequent truss optimization. This will serve as a key technique for enabling the integrated structural design process combining topology optimization and truss optimization. The experiments successfully demonstrated the effectiveness of the three-dimensional structure refinement techniques, and the automatic node search and the bar connectivity determination approaches, when the material usage ratio of the optimal configuration is less than 10%.

References

- [1] A.G.M. Michell, "The Limits of Economy of Material in Framed Structures", *Philosophy Magazine*, 8, 589-597, 1904.
- [2] W.S. Dorn, R.E. Gomory, H.J. Greenberg, "Automatic Design of Optimal Structures", *Journal de Mecanique*, 3, 25-52, 1964.
- [3] M.W. Dobbs, L.P. Felton, "Optimization of Truss Geometry", *Journal Structural Div, ASCE*, 95, 2105-2118, 1969.
- [4] L.A. Schmit, "Structural Design by Systematic Synthesis", *Proceedings of the 2nd Conference on Electronic Computation, ASCE*, 105-122, 1960.
- [5] R.T. Haftka, and R.V. Grandhi, "Structural Shape Optimization- a Survey", *Computer Methods in Applied Mechanics and Engineering*, 57, 91-106, 1986.
- [6] P.Y. Papalambros, M. Chirehdast, "An Integrated Environment for Structural Configuration Design", *Journal of Engineering Design*, 1, 73-96, 1990.
- [7] M.P. Bendsøe, N. Kikuchi, "Generating Optimal Topologies in Structural Design Using a Homogenization Method," *Computer Method in Applied Mechanics and Engineering*, 71, 197-224, 1988.
- [8] C.Y. Lin, J.N. Chou, "A Two-Stage Approach for Structural Topology Optimization," *Advances in Engineering Software*, 30, 261-271, 1999.
- [9] C.Y. Lin, L.S. Chao, "Automated Image Interpretation for Integrated Topology and Shape Optimization," *Structural and Multidisciplinary Optimization*, 20, 125~137, 2000.
- [10] C.Y. Lin, S.H. Lin, "Artificial Neural Network Based Hole Image Interpretation Techniques for Integrated Topology and Shape Optimization," *Computer Method in Applied Mechanics and Engineering*, 194, 3817-3837, 2005.
- [11] C.Y. Lin, Y.H. Chou, "Automated Structural Optimization System for Integrated Topology and Shape Optimization", *Journal of Chinese Institute of Engineers*, 31, 745-756, 2008.
- [12] C.Y. Lin, F.M. Hsu, "An Efficient Algorithm to Obtain the Optimal Topology of Industrial Structural Design Problem", *Journal of Chinese Institute of Engineers*, 31, 17-30, 2008.
- [13] G.N. Vanderplaats, *Numerical Optimization Techniques for Engineering Design*, New York, McGraw-Hill, 1993.
- [14] J. París, F. Navarrina, I. Colominas, M. Casteleiro, "Topology Optimization of Continuum Structures with Local and Global Stress Constraints", *Structural and Multidisciplinary Optimization*, 39, 419-437, 2009.

- [15] J. Rong, J. Yi, "An Optimization Method for Structural Topology Optimization Problems with Stress Constraint and Any Initial Configuration Requirements", IOP Conference Series: Materials Science and Engineering, 10, 2010.
- [16] U. Kirsch, Optimum Structural Design: Concepts, Methods, and Applications, New York, McGraw-Hill, 1981.
- [17] L.J. Leu, C.W. Huang, J.J. Chou, "Topology Optimization of Elastic-plastic Structures", The Chinese Journal of Mechanics, Series A, 19, 397-408, 2003.
- [18] T.Y. Cheng, "Continuum Topology Optimization Based Automatic Optimal Truss Configuration Generation Techniques", Master Thesis, Department of Mechanical Department, National Taiwan University of Science and Technology, Taiwan, R.O.C., 2005.
- [19] C.C. Shen, "2D Truss Design and Optimization Window-Based Platform", Master Thesis, Department of Mechanical Department, National Taiwan University of Science and Technology, Taiwan, R.O.C., 2005.
- [20] S. Zhang, K.S. Fu, "A Thinning Algorithm for Discrete Binary Images," Proceedings of the International Conference on Computer and Application, Beijing, China, 879-886, 1984.
- [21] C.M. Ma, M. Sonka, "A Fully Parallel 3D Thinning Algorithm and Its Applications", Computer Vision and Image Understanding, 64, 420-433, 1996.
- [22] T. Wang, A. Basu, "An Improved Fully Parallel 3D Thinning Algorithm", Department of Computing Science, University of Alberta, Canada, 2005.
- [23] T. Wang, A. Basu, "A Note on a Fully Parallel 3D Thinning Algorithm and Its Applications". Pattern Recognition Letters, 28, 501-506, 2007.
- [24] D. Ballard, C. Brown, Computer Vision, Prentice-Hall, NY, 1992.
- [25] J.B. Jacobsen, N. Olhoff, E. Rønholdt, "Generalized Shape Optimization of Three-dimensional Structures Using Materials with Optimum Microstructures", Mechanics of Materials, 28, 207-225, 1998.